Visualization of Rab5 activity in living cells by FRET microscopy and influence of plasma-membrane-targeted Rab5 on clathrin-dependent endocytosis

Emilia Galperin and Alexander Sorkin*

Department of Pharmacology, University of Colorado Health Sciences Center, Denver, CO 80262, USA
*Author for correspondence (e-mail: alexander.sorkin@uchsc.edu)

Accepted 25 July 2003
Journal of Cell Science 116, 4799-4810 © 2003 The Company of Biologists Ltd
doi:10.1242/jcs.00801

Summary

Rab5 is a small GTPase that controls endocytosis and early endosome dynamics. To visualize active, GTP-loaded Rab5 in living cells, we developed molecular sensors consisting of the Rab5-binding fragments of Rabaptin5 or EEA.1 fused to yellow fluorescent protein (YFP). Interaction of these sensors with GTP-bound Rab5 fused to cyan fluorescent protein (CFP) resulted in fluorescence resonance energy transfer (FRET) between CFP and YFP. Activated Rab5 was detected by FRET microscopy in endosomal compartments and often concentrated in microdomains in the endosomal membrane. Although the plasma membrane-localized activity of Rab5 was not detected by light microscopy, overexpression of a GDP-bound mutant of CFP-Rab5(S34N) inhibited internalization of the epidermal growth factor receptor by retaining receptors in clathrin-coated pits. To test whether the Rab5(S34N) mutant affects endocytosis directly at the plasma membrane, CFP-Rab5 was fused to the plasma membrane targeting sequence of K-Ras containing a CAAX motif. The resulting chimeric CFP-Rab5-CAAX was located mainly in the plasma membrane and was capable of binding GTP as judged by FRET microscopy with the Rabaptin5-based sensor. Interestingly, EEA.1 sensor did not follow activated Rab5-CAAX to the plasma membrane, suggesting that the interaction of EEA.1 with Rab5 plays a secondary role in EEA.1 targeting. Overexpression of CFP-Rab5(S34N)-CAAX prevented endocytosis of receptors by retaining them in coated pits. These data suggest that the dominant-negative effect of the Rab5(S34N) mutant on the late stages of endocytosis can be mediated through the inhibition of cytosol-associated or plasma-membrane-associated rather than endosome-associated regulators of Rab proteins.

Key words: Rab5, Epidermal Growth Factor, EGF, Endocytosis

Introduction

Various macromolecules and viruses enter cells by means of receptor-mediated endocytosis. This process is accomplished in small areas of the plasma membrane coated on the cytoplasmic surface with a clathrin lattice, called clathrin-coated pits. Ligand-receptor complexes destined for internalization are selectively recruited into coated pits followed by coat invagination, constriction and scission of the clathrin-coated vesicle containing cargo (Kirchhausen, 2000). Endocytic vesicles release their clathrin coat and fuse with early endosomes. Internalized ligand-receptor complexes pass through a series of endosomal compartments where they are sorted to different intracellular destinations. Some receptors are recycled back to the plasma membrane with or without the ligand, whereas others are sent to the late endosomal compartment and lysosomes for degradation (Sorkin and von Zastrow, 2002).

Endosomal biogenesis, fusion and maturation are controlled by small GTPases of the Rab family (Zerial and McBride, 2001). Rab5 is located on the cytoplasmic surface of early endosomes, and is a key component of the protein complex responsible for homotypic fusion of early endosomes and cargo sorting in these organelles (Stenmark et al., 1994). Rab5 switches between GTP- and GDP-bound conformations. GTP loading of Rab5 is necessary for Rab5 targeting to early endosomes and interaction with effector proteins. Overexpression of the constitutively active (GTP-loaded) mutant of Rab5 causes dramatic enlargement of early endosomes (Stenmark et al., 1994). Rab5-GTP interacts with, and facilitates, membrane docking of several molecules, such as early endosomal autoantigen 1 (EEA.1), Rabaptin5 and Rabenosin5 (Christoforidis and Zerial, 2000; Lippe et al., 2001). EEA.1 and Rabenosyn5 possess FYVE domains that bind to phosphatidylinositol (3)-phosphate [PtdIns(3)*P*] (Nielsen et al., 2000). Binding to PtdIns(3)*P* in conjunction with Rab5 interaction targets these proteins specifically to early endosomes. Rabaptin5 is a cytosolic protein that is complexed with Rabex5 [Rab5 GDP/GTP exchange factor (GEF)]. The Rabaptin5/Rabex complex is recruited to GTP-loaded Rab5 and positively regulates Rab5 activity by slowing down GTP hydrolysis (Horiuchi et al., 1997).

The function of Rab5 might not be limited to the regulation of early endosome dynamics. Several studies have implicated Rab5 in the process of clathrin-dependent endocytosis. Rab5 is found at the plasma membrane and in coated vesicles, where its activity may regulate the fusion of these vesicles with early endosomes (Bucci et al., 1992). Overexpresion of constitutively active Q79L or dominant-negative S34N Rab5 mutants, respectively, accelerate or inhibit endocytosis of transferrin and epidermal growth factor (EGF) receptors (Bucci

et al., 1992; Stenmark et al., 1994; Barbieri et al., 2000). Studies with Rab5 mutants and Rab5-regulating proteins such as Rab-GDI and Rab5 GTPase-activating protein, RN-tre, also suggest that Rab5 activity is important for clathrin-dependent endocytosis (Lanzetti et al., 2000; Martinu et al., 2002; McLauchlan et al., 1998). By contrast, Ceresa and Schmid (Ceresa and Schmid, 2000) showed that overexpression of the Q79L Rab5 mutant does not alter trafficking of the transferrin receptor (Ceresa et al., 2001). It has been reported that Rab5 is also involved in regulation of fluid-phase endocytosis (Barbieri et al., 2001).

In this study, we used fluorescence resonance energy transfer (FRET) microscopy to visualize directly the activity of fluorescently tagged Rab5 and its interactions with effector proteins in living cells. Similar approaches have been previously developed to observe the activity of other small GTPases, such as Ras and Rac (Jiang and Sorkin, 2002; Kraynov et al., 2000; Mochizuki et al., 2001). A FRET-based sensor was utilized to demonstrate the activity of a Rab5 chimera specifically targeted to plasma membrane (Rab5-CAAX). Interestingly, overexpression of a GDP-bound mutant of Rab5 or Rab5-CAAX protein delayed EGF receptor endocytosis by retaining receptors in clathrin-coated pits, suggesting that Rab5 or a homologous Rab protein might function directly at the plasma membrane during late stages of coated vesicle endocytosis.

Materials and Methods

Reagents

EGF was obtained from Collaborative Research (Bedford, MA). EGF conjugated to rhodamine (EGF-Rh) and human transferrin conjugated to Texas Red (Tfr-TR) were obtained from Molecular Probes (Eugene, OR). Pfu polymerase was purchased from Stratagene (La Jolla, CA). Monoclonal antibodies to GFP were purchased from Zymed Laboratories (South San Francisco, CA). Monoclonal antibodies to Rab5 were purchased from BD Transduction Laboratories (CA).

Plasmids

Human Rab5a, Rab4a and K-Ras4B cDNAs were obtained from Guthrie cDNA Resource Center (Guthrie Research institute, Sayre, PA). Rat β2-YFP cDNA was described previously (Jiang and Sorkin, 2002; Sorkina et al., 2002). Human EEA1 and Rabaptin5 cDNAs were provided by H. Stenmark (Norwegian Radium Hospital, Oslo, Norway) and M. Zerial (Dresden, Germany), respectively. GFP-K44A-Dynamin II was provided by M. McNiven (Mayo Clinic, Rochester, MN). To generate YFP/CFP fusion proteins, Rab5 or Rab4 full-length cDNAs were amplified by PCR and ligated to pEYFP-C1 (Clontech) by using *Bgl*II and *Xho*I restriction sites.

The green fluorescent protein (GFP)-tagged clathrin light chain A (CL_A) construct was provided by L. Green (NIH, Bethesda, MD). To generate YFP-CL_A, full-length CL_A cDNA was ligated to pEYFP-C3 (Clontech) using *Eco*RI and *Xho*I restriction sites. To generate Rabaptin5 YFP/CFP fusion proteins, a fragment corresponding to amino acid residues 551-862 of Rababtin5 (Rab5-binding domain, referred to as R5BD) was amplified by PCR and ligated to pEYFP-N1 (Clontech) using *Sal*I and *Xho*I restriction sites. To generate EEA.1 YFP/CFP fusion proteins, a fragment corresponding to amino acid residues 1306-1411 of EEA.1 (further referred to as EEA1sh) was amplified by PCR and ligated to pEYFP-C3 (Clontech) using *Hind*III and *Bam*HI restriction sites. To generate CFP-Rab5-CAAX fusion proteins, full-length Rab5 was amplified with a 5′ primer that encodes a *Hind*III site and a 3′ primer encompassing a sequence corresponding to the last 20 amino acids of K-Ras4B linker ending with a *Pst*I site. The PCR product was ligated into the *Hind*III/*Pst*I-digested pECFP-C2 vector (Clontech). Point mutations in CFP-Rab5 and CFP-Rab5-CAAX constructs were introduced using the QuickChange site-directed mutagenesis kit (Stratagene). All constructs were verified by dideoxynucleotide sequencing.

Cell culture and transfections

Porcine aortic endothelial (PAE) cells (clone B2) expressing 2×10^5 EGFR/cell (Jiang and Sorkin, 2002) were grown in F12 medium containing 10% fetal bovine serum, and supplemented with antibiotics, glutamine and G418. The transfections of CFP or YFP fusion protein constructs were performed using Effectene (QIAGEN, Hilden, Germany) in six-well plates. For microscopy, cells were replated 24 hours after transfection onto 25 mm glass coverslips. Cells were incubated in serum-free and Phenol Red-free medium containing 0.1% bovine serum albumin (BSA) for 6 hours before experiments. Expression of YFP- and CFP-fused proteins was confirmed by western blotting as described previously (Jiang and Sorkin, 2002).

Fluorescence microscopy

Cells treated or not treated with EGF-Rh or Trf-TR were washed with Ca^{2+}/Mg^{2+}-free phosphate buffered saline (CMF-PBS). For live-cell microscopy, glass coverslips with cells were mounted in a microscopy chamber (Molecular Probes) and imaged at room temperature (RT). Otherwise, the cells were fixed with freshly prepared 4% paraformaldehyde (Electron Microscopy Sciences) for 30 minutes at 4°C.

The fluorescence imaging workstation consisted of a Nikon inverted microscope equipped with a 100× oil immersion objective lens, cooled charge-coupled device SensiCam QE-16MHz (Cooke, Germany), z-step motor, dual filter wheels, and a Xenon 175-W light source, all controlled by SlideBook 3.1 software (Intelligent Imaging Innovation, Denver, CO). The detection of YFP, CFP and rhodamine fluorescence was performed using YFP, CFP and Cy3 filter channels, and an 86004BS dichroic mirror (Chroma, Bratteleboro, VT). Images were acquired using 2×2 binning mode. Typically, Z-stack of 20-30 X-Y optical sections was obtained from fixed cells as previously described (Sorkina et al., 2002). The final arrangement of all images was performed using Adobe Photoshop (Adobe Systems, Mountain View, CA).

FRET measurements

The method of sensitized FRET measurement has been described previously (Sorkin et al., 2000). Briefly, images were acquired sequentially through YFP, CFP and FRET filter channels at RT. Filter sets used were YFP (excitation, 500/20 nm; emission, 535/30 nm); CFP (excitation, 436/10 nm; emission, 470/30 nm) and FRET (excitation, 436/10 nm; emission, 535/30 nm). An 86004BS dichroic mirror (Chroma) was utilized. Images were acquired using 2×2 binning mode and 100-250 ms integration times. The background was subtracted from the raw images prior to carrying out FRET calculations. Corrected FRET ($FRET^C$) was calculated on a pixel-by-pixel basis for the entire image using the following equation.

$$FRET^C = FRET - (0.50 \times CFP) - (0.02 \times YFP), \quad (1)$$

where FRET, YFP and CFP correspond to background-subtracted images of cells co-expressing CFP and YFP acquired through the FRET, YFP and CFP channels, respectively. 0.5 and 0.02 are the fractions of bleed-through of CFP and YFP fluorescence, respectively, through the FRET channel. Bleed-through coefficients of CFP and YFP fluorescence were slightly overestimated, as described in (Sorkin et al., 2000), which can result in some underestimation of $FRET^C$ and negative $FRET^C$ values.

As an additional approach, $FRET^C$ values were calculated from the mean fluorescence intensities for each selected subregion of the image containing individual endosomes, ruffles and diffuse fluorescence areas according to Eqn 1. Normalized sensitized FRET (FRETN) values for individual cellular compartments were calculated according to the following equation.

$$FRETN = FRET^C/(YFP \times CFP), \quad (2)$$

where $FRET^C$, CFP and YFP are the mean intensities of $FRET^C$, CFP and YFP fluorescence in the selected subregion of the image. In these calculations, the fluorescence intensity of CFP was underestimated because of donor fluorescence quenching due to FRET. This quenching of donor fluorescence was calculated from $FRET^C$ values using the conversion coefficient G (3.2 in all experiments) as described (Gordon et al., 1998) and was found to be about 5-10% of CFP fluorescence intensities. Therefore, the underestimation of CFP fluorescence did not significantly affect FRETN values.

The maximum high FRETN values ($5.99\times10^{-4}\pm0.23\times10^{-4}$) were obtained in PAE cells expressing a chimeric CFP-YFP protein consisting of CFP and YFP connected by a 16-amino acid residue linker (Vanderklish et al., 2000). Using a photobleaching FRET method, in which the increase of donor fluorescence upon acceptor photobleaching is measured, the FRET efficiency (E) was determined in cells, in which $FRET^C$ values had been measured, using the equation:

$$E = 1 - CFP_B/CFP_A, \quad (3)$$

where CFP_B and CFP_A are the integrated intensities of CFP images of the whole cells measured, respectively, before and after YFP photobleaching (CFP_B is analogous to CFP in Eqn 1). YFP was photobleached by irradiation through a 535/20 nm bandpass filter. The mean value of E was 32.6%. Because CFP_A is significantly larger than CFP_B owing to high FRET efficiency, FRETN values for CFP-YFP protein were calculated according to the modified Eqn 2:

$$FRETN = FRET^C/(YFP \times CFP_A). \quad (4)$$

$FRET^C$ images are presented in a pseudocolor mode. $FRET^C$ intensity is displayed stretched between the low and high renormalization values, according to a temperature-based lookup table with blue (cold) indicating low values and red (hot) indicating high values. To eliminate distracting data from regions outside of cells, the CFP channel was used as a saturation channel, and the $FRET^C$ images were displayed as CFP intensity-modulated images. In these images, data with CFP values greater than the high threshold of the saturation channel are displayed at full saturation, whereas data values below the low threshold are displayed with no saturation (i.e. black). All calculations were performed using the channel math and FRET modules of the Slidebook software.

Results

Visualization of GTP-bound form of Rab5 in living cells

To study Rab5 activity and interactions in living cells, CFP- and YFP-fusion proteins of Rab5a were prepared (Fig. 1A). Identical fluorescent-protein-tagged fusions of Rab5 have been previously characterized in several studies (Barbieri et al., 2000; Roberts et al., 1999; Roberts et al., 2000). In order to visualize the GTP-bound form of Rab5, fluorescent sensors were generated based on two known interactors of Rab5-GTP, Rabaptin5 and early endosomal antigen 1 (EEA.1) (Fig. 1A).

Rabaptin5 binds directly to the GTP-loaded form of Rab5 in vitro and is recruited to early endosomes in a Rab5-dependent manner (Stenmark et al., 1995). The Rab5-interacting domain of Rabaptin5 (referred to as R5BD) was mapped in in vitro experiments to the C-terminal residues 551-886 of Rabaptin5 (Vitale et al., 1998). To generate a FRET-based sensor for active, GTP-bound Rab5, a YFP-fusion protein of R5BD was constructed (Fig. 1A).

EEA.1 is a component of the endosomal fusion machinery that binds to the GTP-loaded form of Rab5. A 30-amino acid region upstream of the FYVE domain of EEA.1 was shown to be essential for Rab5 binding in vitro, although the functional FYVE domain was also required for efficient interaction (Lawe et al., 2000). To generate an EEA.1-based sensor for Rab5-GTP (YFP-EEA.1sh), YFP was fused to the amino acid residues 1306-1411 of EEA.1 (Fig. 1A). Such a fusion protein

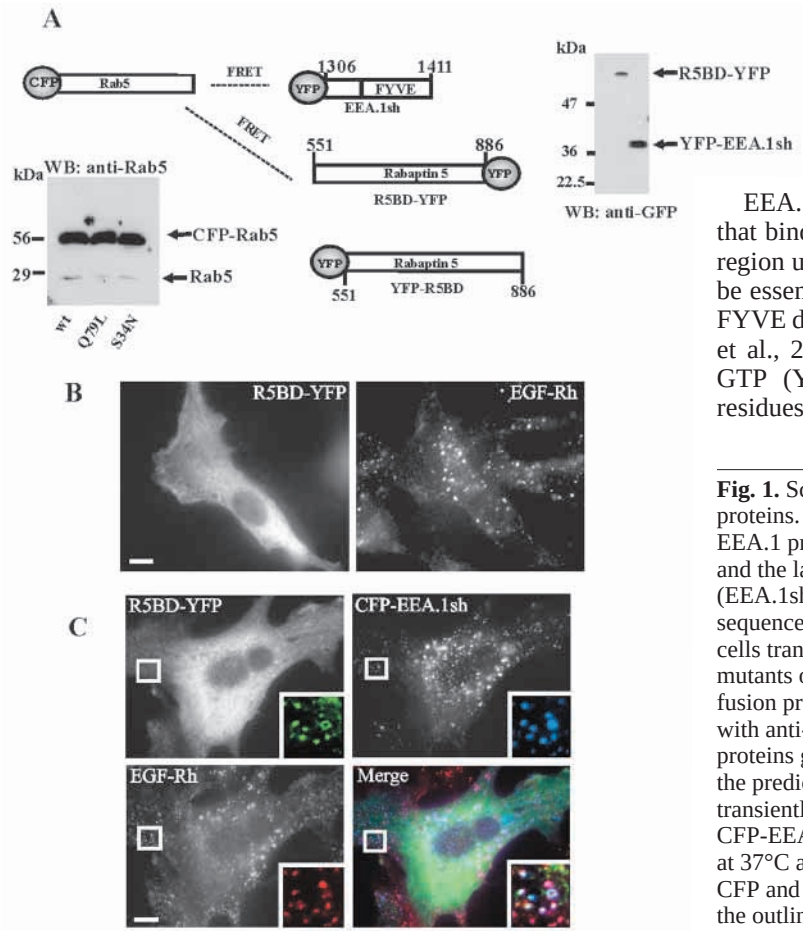

Fig. 1. Schematic representation and immunodetection of fusion proteins. (A) Depicted are Rab5, and fragments of Rabaptin5 and EEA.1 proteins fused to CFP/YFP at the N- or C-terminus. The first and the last amino acid residues in Rabaptin 5 (R5RB) and EEA.1 (EEA.1sh) fragments are numbered according to the full-length sequences. The FYVE domain of EEA.1 is indicated. PAE/EGFR cells transiently expressing wild-type (wt), Q79L or S34N CFP-Rab5 mutants or YFP-EEA.1 and R5BD-YFP were lysed, and CFP/YFP-fusion proteins present in lysates were detected by western blotting with anti-Rab5 or anti-GFP antibodies, respectively. All fusion proteins generated in this work migrated on SDS-PAGE according to the predicted molecular masses. (B and C) PAE/EGFR cells transiently expressing R5BD-YFP alone (B) or together (C) with CFP-EEA.1sh were incubated with 1 ng/ml EGF-Rh for 10 minutes at 37°C and fixed. EGF-Rh, CFP and YFP were detected using Cy3, CFP and YFP filter channels. Insets in (C) show an enlargement of the outlined regions. Bars, 10 μm.

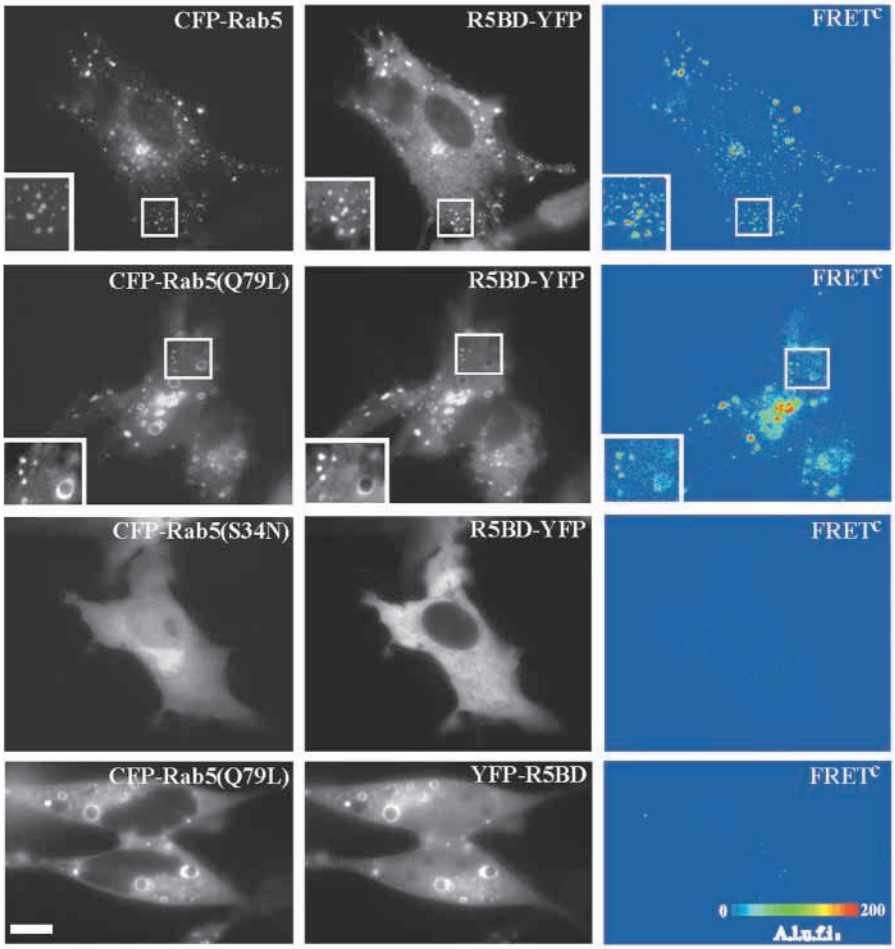

Fig. 2. Detection of GTP-bound Rab5 in living cells. CFP-Rab5, CFP-Rab5(Q79L) or CFP-Rab5(S34N) were co-expressed with R5BD-YFP or YFP-R5BD in PAE/EGFR cells. YFP, CFP and FRET images were obtained from living cells at RT. $FRET^C$ was calculated as described in Materials and Methods, and presented as pseudocolor images. Insets show an enlargement of the outlined regions. A.l.u.f.i., arbitrary linear units of fluorescence intensity. Bar, 10 μm.

has been previously characterized and used as an early endosomal marker (Gaullier et al., 1998; Lawe et al., 2000).

The localization of YFP/CFP-fused proteins was examined in A-431, HeLa and PAE cells. Despite differences in cell morphology and the expression levels of fusion proteins, similar results were observed in all these cell lines. CFP-Rab5 and YFP-EEA.1sh proteins were concentrated in endosomes. The R5BD-YFP fusion protein displayed cytosolic distribution in the absence of Rab5 overexpression (Fig. 1B). In this study, PAE cells were used as the preferred expression system because they have minimal autofluorescence background and flattened cell shape, which allows clear visualization of organelles and other structures.

As shown in Fig. 1B,C, expression of R5BD-YFP alone or together with CFP-EEA.1sh did not visibly affect the endocytosis of EGF-rhodamine (EGF-Rh) in PAE cells expressing EGF receptors (PAE/EGFR). Interestingly, when R5BD-YFP was co-expressed with CFP-EEA.1sh, a pool of R5BD-YFP was recruited to endosomes containing EGF-Rh and CFP-EEA.1sh (Fig. 1C). It is possible that the recruitment to endosomes of EEA.1sh protein containing Rab5-GTP binding sites might increase the concentration of endogenous Rab5-GTP on the endosomal membrane, and consequently recruit R5BD-YFP to these endosomes.

To test directly whether R5BD can bind Rab5 on the endosomal membrane, R5BD-YFP was co-expressed with CFP-Rab5. Co-expression of these fusion proteins resulted in the recruitment of a substantial pool of R5BD-YFP to CFP-Rab5-containing endosomes (Fig. 2). To examine whether R5BD-YFP is bound to CFP-Rab5, sensitized FRET efficiencies between CFP and YFP ($FRET^C$) were measured on a pixel-by-pixel basis as described in Materials and Methods. As seen in Fig. 2, $FRET^C$ images revealed strong energy transfer between CFP-Rab5 and R5BD-YFP, suggesting that these two proteins form a complex in endosomes.

Rab5, as other GTPases, switches between GTP- and GDP-bound conformations. To test the specificity of Rab5-GTP detection by the R5BD-YFP sensor, GTP- and GDP-bound mutants of CFP-Rab5 were generated. The Q79L mutation results in significant reduction of GTP hydrolysis by Rab5, thus keeping Rab5 in a GTP-bound state. The S34N mutation yields Rab5 protein that preferentially binds GDP over GTP, thus keeping Rab5 in an inactive state (Stenmark and Olkkonen, 2001). The properties of these Rab5 mutants have been previously reproduced with CFP/YFP-fused Rab5 proteins (Barbieri et al., 2000; Sonnichsen et al., 2000).

Co-expression of the CFP-Rab5(Q79L) mutant and R5BD-YFP resulted in the appearance of enlarged endosomes, massive recruitment of R5BD-YFP to Rab5-containing endosomal complexes and strong $FRET^C$ signals (Fig. 2). By contrast, co-expression of the CFP-Rab5(S34N) mutant and R5BD-YFP fusion proteins did not result in the recruitment of either R5BD-YFP or CFP-Rab5(S34N) to endosomes (Fig. 2). In some cells, CFP-Rab5(S34N) was seen associated with distinct organelles often located in the perinuclear area of the cell. No positive $FRET^C$ signal was observed in cells co-expressing CFP-Rab5(S34N) with R5BD-YFP (Fig. 2). These data suggest that the interaction of Rab5 and R5BD fusion proteins depends on GTP-loading of Rab5, thus validating the use of R5BD protein as a sensor of Rab5 activity.

Interestingly, when YFP was fused to the N-terminus of R5BD (YFP-R5BD, Fig. 1), this protein was recruited to endosomes in a Rab5-dependent manner and to an extent similar to that observed for R5BD-YFP (Fig. 2). However, positive FRET signals were not detected despite colocalization of YFP-R5BD with CFP-Rab5 or CFP-Rab5(Q79L) in endosomes (Fig. 2). This observation suggests that, when forming a complex on the endosomal membrane, the

Table 1. Mean FRETN values calculated for individual compartments and regions of cells*

Protein combination	Cellular compartment	$FRETN^C$ (10^{-4})†
Rab5 wt+R5BD-YFP	Endosomes	1.88±0.25 (*n*=37)
Rab5(Q79L)+R5BD-YFP	Endosomes	1.67±0.13 (*n*=34)
Rab5(S34N)+R5BD-YFP	Diffused fluorescence, perinuclear structures	–0.02±0.1 (*n*=15)
Rab5(Q79L)+YFP-R5BD‡	Endosomes	–0.42±0.12 (*n*=12)
Rab5(Q79L)+YFP-EEA.1sh§	Endosomes	2.11±0.17 (*n*=26)
Rab5(Q79L)-CAAX+YFP-R5BD	Plasma membrane	0.82±0.15 (*n*=9)
CFP-YFP¶	Diffused fluorescence	5.99±0.23 (*n*=4)

*Defined cell regions with the molar ratio of CFP/YFP fluorescence from 2-3 were used for calculations.

†Mean value±s.e.; each FRETN value was obtained for several selected regions in the individual cell and 5-10 cells were analyzed for each FRET pair. The cells were selected from at least five independent experiments.

‡Negative control: cells expressing proteins that are colocalized but do not FRET.

§Defined cell regions with the molar ratio of CFP/YFP fluorescence from 1-2 were used for calculations.

¶Measurements were performed for whole cells as described in Materials and Methods.

fluorescent protein attached to the N-terminus of Rab5 is in close proximity to, and oriented favorably for, FRET with the C-terminus of Rabaptin5 but not theN-terminus of Rabaptin5.

Because the intensity of energy transfer depends of the amounts of donor and acceptor capable of interaction, $FRET^C$ values were divided by the product of YFP and CFP intensities on a pixel-by-pixel basis to obtain normalized $FRET^C$ (FRETN) values for individual endosomes and various regions of the cells (see Materials and Methods). FRETN values correlate with the equilibrium binding constant for the measured interaction and may, therefore, serve as a measure of the relative affinity of the interaction (Gordon et al., 1998). FRETN values in cells expressing R5BD-YFP/CFP-Rab5 were similar to these values in cells expressing R5BD-YFP/CFP-Rab5(Q79L) and were significantly higher than in cells expressing R5BD-YFP/CFP-Rab5(S34N) or YFP-R5BD/CFP-Rab5 (Table 1). The negative FRETN values obtained for control CFP-YFP pairs are owing to slight overestimation of the bleed-through coefficients during $FRET^C$ calculations (see Materials and Methods).

As an additional control to confirm that R5BD-YFP localization and interactions in endosomes are specific for Rab5, the CFP-Rab4 fusion protein was transiently co-expressed with R5BD-YFP in PAE/EGFR cells. As shown in Fig. 3A, the R5BD-YFP fusion protein was not associated with Rab4-containing endosomes and no $FRET^C$ signal was observed. Taken together, the data presented in Figs 2 and 3A show that R5BD-YFP can serve as a specific sensor molecule for detecting Rab5 activity in living cells.

Detection of Rab5 interaction with EEA.1sh by FRET

To test whether the EEA.1 Rab5-binding domain can serve as a sensor for Rab5-GTP, YFP-EEA.1sh protein was co-expressed with CFP-Rab5 in PAE/EGFR cells. Both proteins were well colocalized in endosomes (Fig. 3B). Mutation of His1372 to tyrosine in the PtdIns(3)*P*-binding pocket of the FYVE domain (Kutateladze and Overduin, 2001) prevented endosomal targeting of YFP-EEA.1sh, thus confirming that this protein is recruited to endosomes by a mechanism similar to that responsible for the endosomal localization of full-length EEA.1 (data not shown). Strong $FRET^C$ signals were detected indicative of the interaction of Rab5 and EEA.1sh fusion proteins (Fig. 3B, Table 1). By contrast, no FRET was observed between CFP-Rab4 with YFP-EEA.1sh proteins, although these proteins were partially colocalized in some endosomes (Fig. 3A). Moreover, no FRET was detected in cells expressing CFP-Rab5(S34N) and YFP-EEA.1sh (Fig. 3B). These experiments demonstrated that EEA.1sh can be used as a sensor of Rab5-GTP in endosomes of living cells.

Interestingly, $FRET^C$ signals were concentrated in the confined domains of the endosomal membrane (Fig. 3C), which is consistent with sub-compartmental organization of Rab5/EEA.1 complexes in endosomes (de Renzis et al., 2002). By contrast, R5BD-YFP/Rab5 $FRET^C$ was observed along all membrane of endosomes, suggesting that Rab5-GTP is present on endosomal membrans in significant amounts outside of 'Rab5/EEA.1 domains'. Thus, EEA.1sh does not detect all activated Rab5 and is, therefore, a less useful sensor for Rab5 activity. Moreover, because EEA.1sh contains a FYVE domain, it was associated with endosomes even in the presence of the Rab5(S34N) mutant, albeit at a lesser extent than in the absence of Rab5(S34N) (Fig. 3B).

Rab5 influence on EGF receptor internalization

The role of Rab5 in endosomal fusion is well established in studies in vitro and in vivo (Stenmark and Olkkonen, 2001; Zerial and McBride, 2001). The sites of Rab5 action during clathrin-mediated endocytosis remain to be defined. We examined the ability of CFP-Rab5 mutants to influence EGF receptor endocytosis in PAE cells. Because only a fraction of the PAE/EGFR cell population expressed Rab5 fusion proteins in significant amounts, single cell microscopy analysis of EGF-Rh endocytosis was utilized. PAE/EGFR cells overexpressing CFP-Rab5 or its mutants were stimulated with 1 ng/ml EGF-Rh for 10 minutes at 37°C. Under these conditions, about 70-80% of EGF-Rh/receptor complexes are internalized (Jiang et al., 2003). A low concentration of EGF-Rh was used to avoid potential saturation of the clathrin-dependent endocytic pathway (Sorkina et al., 2002). The cells were also co-transfected with the β2 subunit of the clathrin adaptor AP-2 complex (β2-YFP), a marker of clathrin pits and vesicles (Sorkina et al., 2002). The localization of EGF-Rh relative to Rab5 and coated pits was then examined by direct fluorescence of labeled proteins to circumvent problems arising from cell permeabilization and the use of immunostaining.

A microscopic analysis revealed that EGF-Rh/receptor complexes were colocalized with CFP-Rab5 (Fig. 4A) or CFP-Rab5(Q79L) (data not shown) in endosomes. A small amount of EGF-Rh was also found colocalized with β2-YFP. By contrast, in cells overexpressing the CFP-Rab5(S34N) fusion protein, very little, if any, EGF-Rh was seen in large vesicular structures (Fig. 4A). Instead, EGF-Rh was concentrated in small dots often colocalized with β2-YFP dots in the bottom and top optical sections of the cells. This pattern of EGF-Rh distribution in cells overexpressing CFP-Rab5(S34N) was reminiscent of EGF-Rh distribution in cells expressing the dominant-negative K44A dynamin-2 mutant. The K44A mutant is incorporated into coated pits and blocks

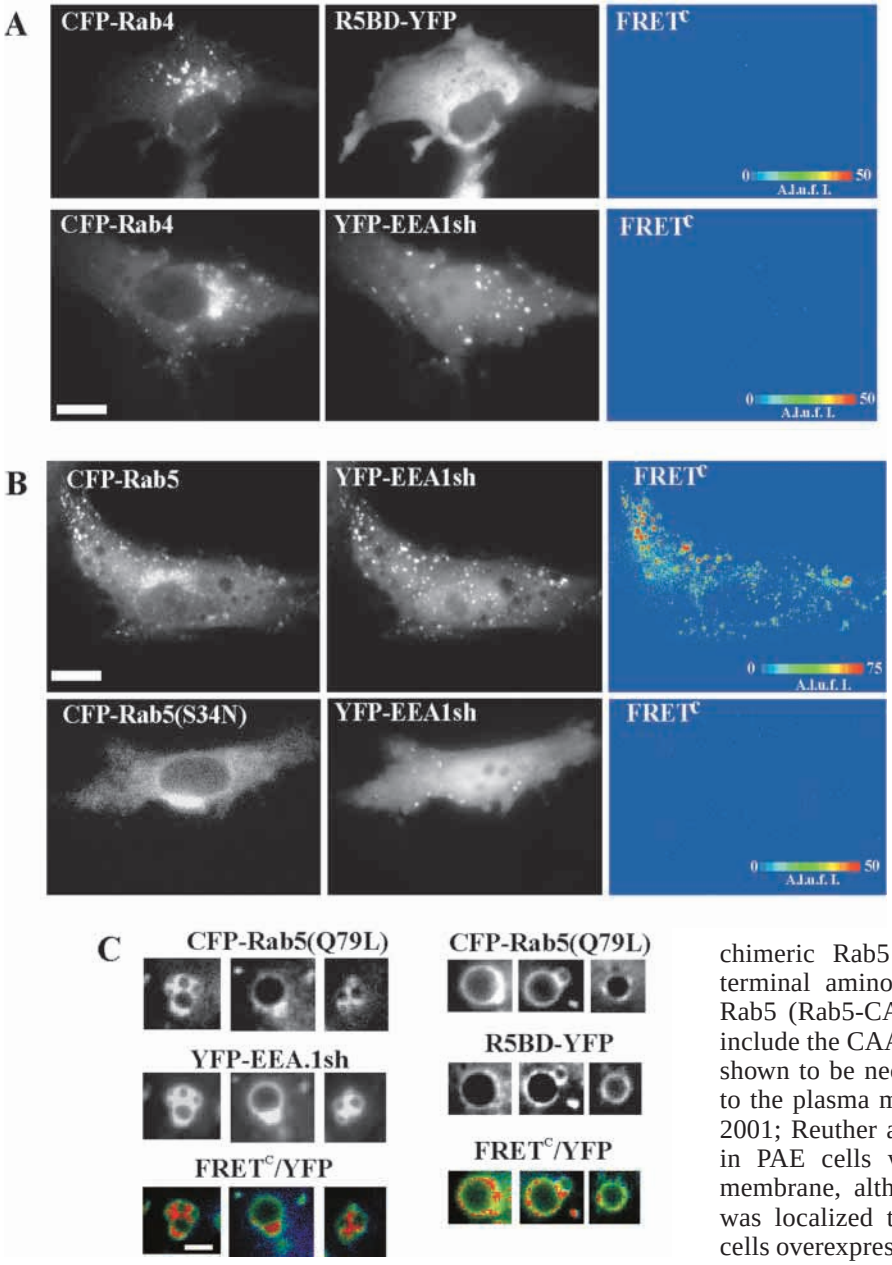

Fig. 3. Specificity of R5BD-YFP and YFP-EEA.1sh sensors for Rab5. (A) CFP-Rab4 was co-expressed with R5BD-YFP or YFP-EEA.1sh in PAE/EGFR cells. (B) CFP-Rab5 or CFP-Rab5(S34N) were co-expressed with YFP-EEA.1sh in PAE/EGFR cells. YFP, CFP and FRET images were obtained from living cells at RT. $FRET^C$ images were calculated as described in Materials and Methods, and presented as pseudocolor images. A.l.u.f.i., arbitrary linear units of fluorescence intensity. Bars (A and B), 10 μm. (C) Gallery of high-magnification images shows individual endosomes or tethered endosomes in cells co-expressing CFP-Rab5(Q79L) and YFP-EEA.1sh or R5BD-YFP. FRET images are presented as pseudocolor intensity-modulated images ($FRET^C$/CFP). Bar, 2 μm.

endocytosis by affecting the constriction of the coat (Damke et al., 1994). Accordingly, EGF-Rh was not accumulated in endosomal compartments but remained colocalized with Dynamin-K44A-GFP at the plasma membrane (Fig. 4B). These data suggest that CFP-Rab5(S34N), similar to the K44A dynamin mutant, slows down the endocytosis of EGF receptors by inhibiting the movement of receptors from coated structures to endosomes.

Targeting of Rab5 to the plasma membrane

The dominant-negative effect of CFP-Rab5(S34N) on clathrin-dependent endocytosis could be mediated directly by sequestering Rab5-regulating proteins, such as GEFs, operating at the plasma membrane or indirectly, through effects on sorting processes in endosomes. Inspection of the localization of Rab5 fusion proteins and their activity by fluorescence microscopy in several types of cells revealed that Rab5 was exclusively localized to endosomes (Figs 2-4). However, the sensitivity of our imaging system might not be sufficient to detect small amounts of Rab5 in the plasma membrane. We therefore tested whether Rab5 can be activated when targeted to the plasma membrane and whether a dominant-negative mutant of plasma-membrane-targeted Rab5 is an effective inhibitor of endocytosis. To this end, a chimeric Rab5 protein was generated, in which 20 C-terminal amino acid residues of K-Ras4B were fused to Rab5 (Rab5-CAAX, Fig. 5A). These residues of K-Ras4B include the CAAX motif and a polylysine sequence that were shown to be necessary and sufficient for targeting of K-Ras to the plasma membrane (Hancock et al., 1990; Prior et al., 2001; Reuther and Der, 2000). CFP-Rab5-CAAX expressed in PAE cells was predominantly targeted to the plasma membrane, although a small pool of the chimeric protein was localized to the endomembrane system. Interestingly, cells overexpressing CFP-Rab5(Q79L)-CAAX had numerous ruffles and pseudopodia that were illuminated by the Rab5 fusion protein (Fig. 5B). CFP-Rab5(S34N)-CAAX was also located mostly at the plasma membrane (see below, Fig. 6).

To test whether CFP-Rab5-CAAX is present in a GTP-bound form, a FRET assay, described above (Figs 2 and 3), was utilized. CFP-Rab5(Q79L)-CAAX was co-expressed with R5BD-YFP or YFP-EEA.1sh, respectively. R5BD-YFP was well colocalized with CFP-Rab5(Q79L)-CAAX in the plasma membrane, particularly in ruffle-like structures, where a strong positive $FRET^C$ signal was detected (Fig. 5B, Table 1). Similar colocalization and energy transfer were observed in cells expressing wild-type CFP-Rab5-CAAX and R5BD-YFP, although the extent of colocalization and $FRET^C$ signals were less than in cells expressing CFP-Rab5(Q79L)-CAAX (data not shown). As expected, membrane recruitment of R5BD-YFP protein in cells expressing CFP-Rab5(S34N)-CAAX was not observed (data not shown).

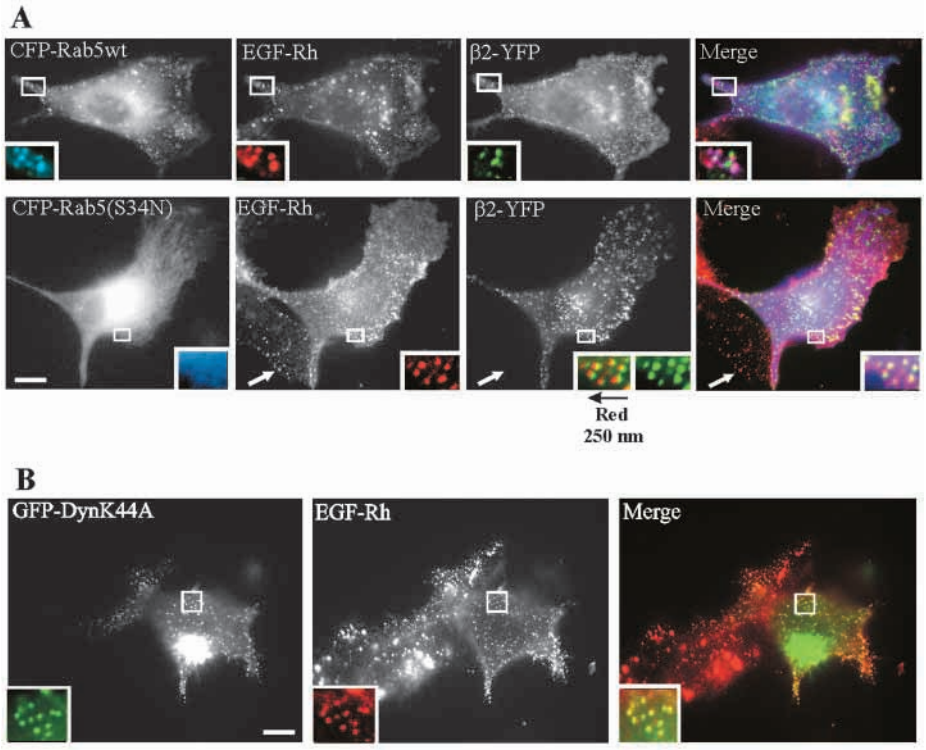

Fig. 4. Effect of Rab5 mutant overexpression on EGF receptor internalization. (A) Wild-type CFP-Rab5 (wt) and CFP-Rab5(S34N) mutant were transiently co-expressed with β2-YFP in PAE/EGFR cells. The cells were incubated with 1 ng/ml EGF-Rh for 10 minutes at 37°C and fixed. EGF-Rh, YFP and CFP were detected using Cy3, YFP and CFP filter channels. Optical sections from the bottom of the cells are shown. 'Yellow' signifies colocalization of YFP and rhodamine fluorescence. 'Cyan' signifies colocalization of CFP and rhodamine fluorescence. Insets show an enlargement of the outlined regions. An additional inset (lower panel, β2-YFP image) shows the merge image of EGF-Rh and β2-YFP, in which the EGF-Rh image (red) was left-shifted 4 pixels (250 nm) to allow better visualization of colocalization of red and green dots. The arrow points to a cell that does not express CFP-Rab5(S34N) and displays typical endosomal localization of EGF-Rh. The images are representative of at least four independent experiments. Bar, 10 μm. (B) GFP-dynamin mutant (DynK44A) was transiently expressed in PAE/EGFR cells. Cells were incubated with 1 ng/ml EGF-Rh for 10 minutes at 37°C. EGF-Rh and GFP-dynamin were detected using Cy3 and GFP filter channels. Insets show an enlargement of the outlined regions. 'Yellow' signifies colocalization of GFP and rhodamine fluorescence. The images are representative of at least four independent experiments. Bar, 10 μm.

When Rab5(Q79L)-CAAX was co-expressed with YFP-EEA.1sh, the colocalization and interaction of the two proteins were observed only in endosomal structures (Fig. 5B). No plasma membrane localization of YFP-EEA.1sh was observed. These data suggest that the FYVE domain bears the primary endosome-targeting signal of EEA.1, whereas the interaction with Rab5 might play an additional role in the formation of Rab5/EEA.1 complexes. The data presented in Fig. 5B indicate that CFP-Rab5-CAAX binds R5BD and EEA.1sh in a GTP-dependent manner, suggesting that Rab5-CAAX is capable of GTP binding and, therefore, interaction with the plasma membrane and cytosolic Rab5 effectors.

Influence of Rab5-CAAX on clathrin-dependent internalization

To test whether CFP-Rab5-CAAX overexpression influences EGF receptor internalization through clathrin-coated pits, PAE/EGFR cells were transiently transfected with wild-type or mutant CFP-Rab5-CAAX. The cells were also co-transfected with β2-YFP to mark coated pits. Fig. 6 demonstrates that, after incubation of cells expressing wild-type CFP-Rab5-CAAX or CFP-Rab5(Q79L)-CAAX mutant with 1 ng/ml EGF-Rh for 10 minutes at 37°C, EGF-Rh was accumulated in endosomes. Endosomes were often concentrated in the perinuclear area, and occasionally contained CFP-Rab5-CAAX but did not overlap with β2-YFP. There was no difference in the pattern of EGF-Rh distribution between Rab5-CAAX-expressing and not expressing cells.

By contrast, in cells expressing CFP-Rab5(S34N)-CAAX, EGF-Rh did not display significant accumulation in endosomes (Fig. 6). Instead, most of EGF-Rh was concentrated in small dots distributed throughout the cell and often colocalized with β2-YFP. Essentially, similar results were obtained when the clathrin light chain A tagged with YFP (YFP-CL_A) was used as a marker of coated pits and vesicles (Fig. 7). These data indicated that the CFP-Rab5(S34N)-CAAX chimera, similar to CFP-Rab5(S34N) and K44A dynamin (Fig. 4), inhibits the steps of the endocytic process after receptor recruitment and before uncoating of the coated vesicle and its fusion with endosomes.

To test whether Rab5(S34N)-CAAX specifically affects EGF receptor endocytosis or also inhibits endocytosis of other cargo through the clathrin pathway, the internalization of transferrin receptors was analyzed. The inhibitory effect of Rab5(S34N) mutant on transferrin uptake was previously reported (Barbieri et al., 2000; Stenmark et al., 1994) and observed in our experiments (data not shown). As shown in Fig. 8A, Tfr-TR (5 μg/ml) did not accumulate in endosomes of PAE cells expressing CFP-Rab5(S34N)-CAAX. Most of Tfr-TR was located in small dots distributed throughout the cell (Fig. 8A). Several examples of colocalization of Trf-TR and β2-YFP are shown in Fig. 8B. Although not all β2-YFP dots contained Trf-TR, most Trf-TR dots overlapped with β2-YFP-labeled coated pits.

By contrast, Trf-TR was rapidly internalized into endosomal structures and often accumulated in the juxta-Golgi recycling compartment in cells expressing wild-type CFP-Rab5-CAAX (Fig. 8A). After 10 minutes of continuous internalization, very little, if any, Trf-TR was detected in

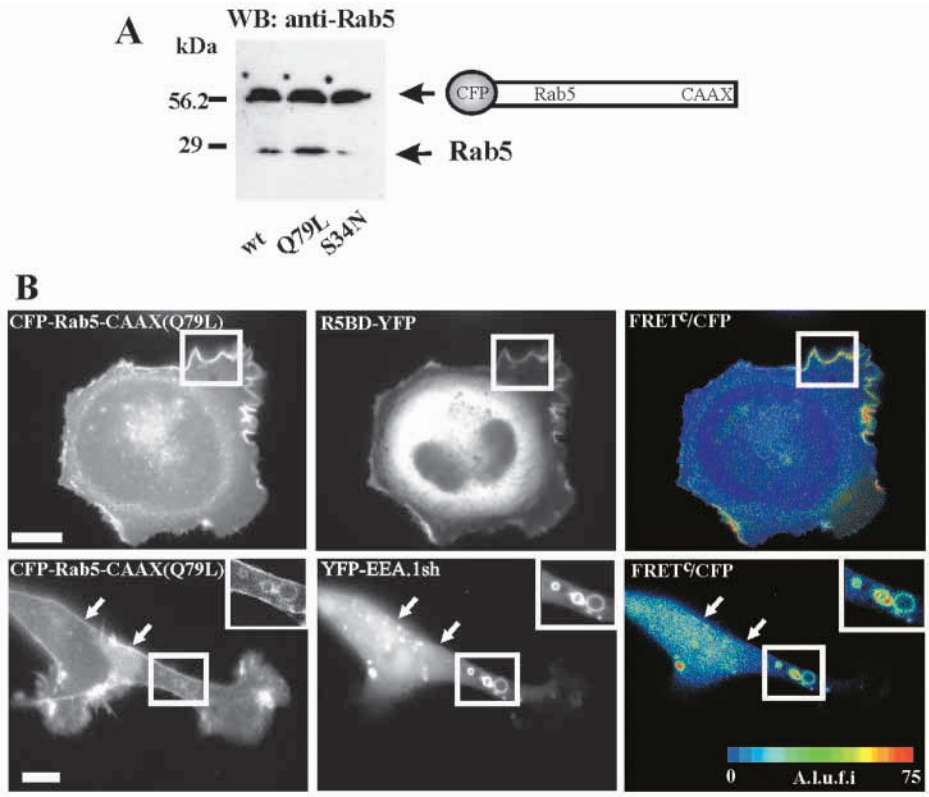

Fig. 5. Detection of Rab5-CAAX activity in the plasma membrane. (A) Schematic representation and immunodetection of fusion proteins. Depicted is CFP-Rab5 protein fused to the 20-residue CAAX module of K-Ras4B at the C-terminus (CFP-Rab5-CAAX). PAE/EGFR cells transiently expressing CFP-Rab5-CAAX or its mutants, Q79L and S34N, were lysed, and the CFP-fusion proteins present in lysates were detected by western blotting with anti-Rab5 antibodies. All fusion proteins migrated on SDS-PAGE according to predicted molecular masses. (B) CFP-Rab5(Q79L)-CAAX was co-expressed with R5BD-YFP or YFP-EEA.1sh in PAE/EGFR cells. YFP, CFP and $FRET^C$ images were obtained as in Fig. 2. Calculated FRET images presented as pseudocolor intensity-modulated images ($FRET^C$/CFP) (see Materials and Methods). Insets show an enlargement of the outlined regions. Arrows point to the absence of YFP-EEA.1sh associated with CFP-Rab5(Q79L)-CAAX at the plasma membrane. A.l.u.f.i., arbitrary linear units of fluorescence intensity. Bars, 10 μm.

coated pits labeled by β2-YFP. There was no difference in the pattern of Tfr-TR distribution between CFP-Rab5-CAAX-expressing and not expressing cells. Altogether, the data presented in Figs 6-8 indicate that the CFP-Rab5(S34N)-CAAX chimera does not prevent the recruitment of cargo into coated pits but slows down the late stages of clathrin-mediated endocytosis.

Discussion

A growing number of studies have explored the potential of FRET microscopy to visualize interactions of proteins in living cells (Zhang et al., 2002). FRET-based genetically encoded sensors have been developed to visualize the activities of intracellular enzymes, including small GTPases of the Ras superfamily (Hahn and Toutchkine, 2002). Two types of

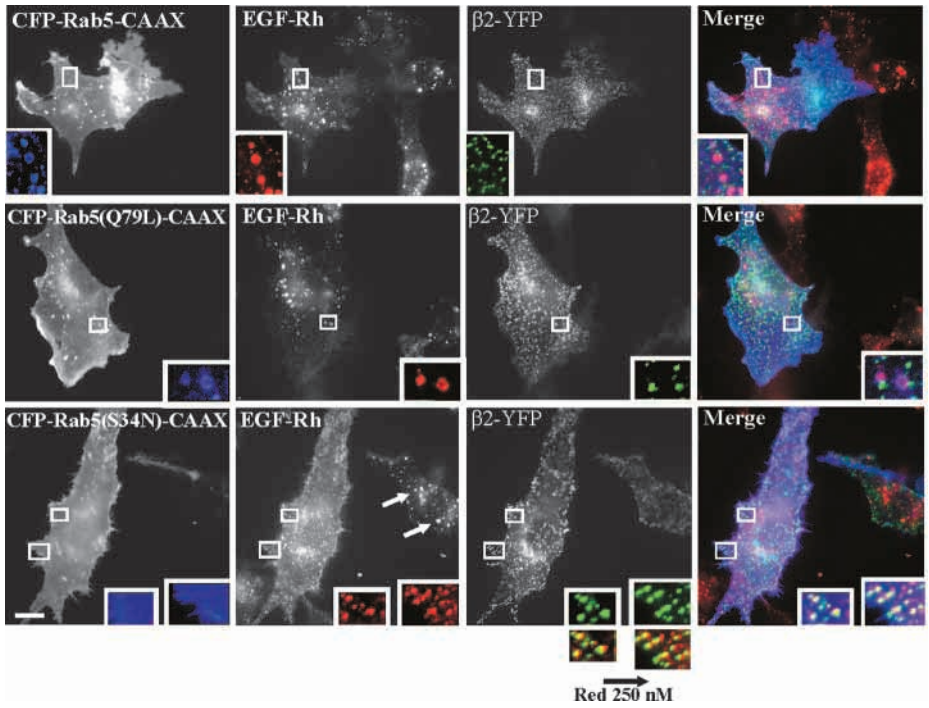

Fig. 6. Effect of CFP-Rab5-CAAX on EGF receptor endocytosis. CFP-Rab5-CAAX, CFP-Rab5(Q79L)-CAAX and CFP-Rab5(S34N)-CAAX were transiently co-transfected with β2-YFP in PAE/EGFR cells. The cells were incubated with 1 ng/ml EGF-Rh for 10 minutes at 37°C and fixed. EGF-Rh, YFP and CFP were detected using Cy3, YFP and CFP filter channels. Optical sections close to the bottom of the cell are shown. 'Yellow' signifies colocalization of YFP and rhodamine fluorescence. 'Cyan' signifies colocalization of CFP and rhodamine fluorescence. Insets show an enlargement of the outlined regions. Additional insets (lower panel, β2-YFP image) show the merge images of EGF-Rh and β2-YFP, in which the EGF-Rh image (red) was right-shifted 4 pixels (250 nm) to allow better visualization of colocalization of red and green dots. The arrows point to a cell that does not express CFP-Rab5(S34N)-CAAX and that displays typical endosomal localization of EGF-Rh. Note colocalization of EGF-Rh with CFP-Rab5(Q79L)-CAAX and CFP-Rab5-CAAX in endosomes is seen as 'donut-shape' structures. Bar, 10 μM.

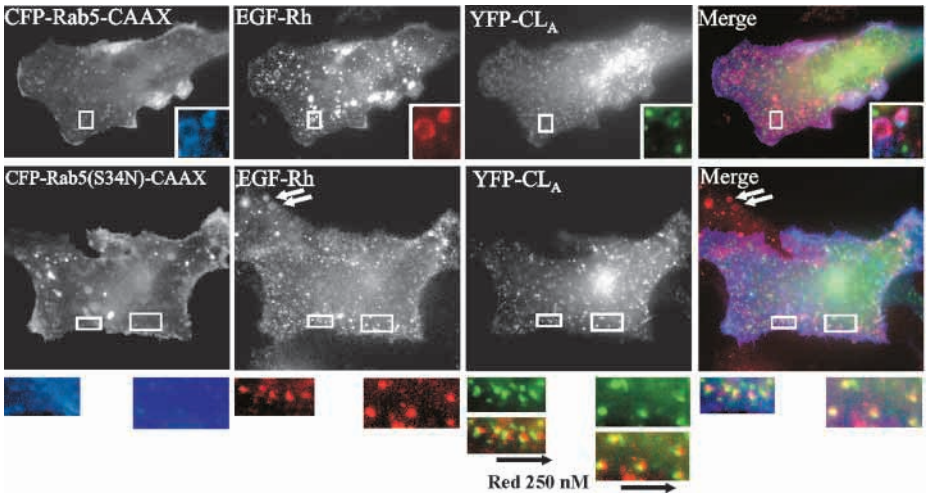

Fig. 7. Colocalization of clathrin and EGF-Rh in cells expressing the dominant-negative Rab5-CAAX mutant. CFP-Rab5-CAAX and CFP-Rab5(S34N)-CAAX were transiently co-transfected with YFP-CL$_A$ in PAE/EGFR cells. The cells were incubated with EGF-Rh as in Fig. 6. EGF-Rh, YFP and CFP were detected using Cy3, YFP and CFP filter channels. 'Yellow' signifies colocalization of YFP and rhodamine fluorescence, whereas 'cyan' signifies colocalization of CFP and rhodamine fluorescence. Insets show an enlargement of the outlined regions. Additional insets below the YFP image show the merge image of EGF-Rh and β2-YFP, in which the EGF-Rh image (red) was right-shifted 4 pixels (250 nm) to allow better visualization of colocalization of red and green dots. The arrows show an example of EGF-Rh-containing endosomes in a cell that does not express CFP-Rab5(S34N)-CAAX.

strategies were employed to design these molecular sensors, both relying on monitoring the interaction between a fragment of the effector molecule binding to a GTPase and a GTPase itself. These two proteins were either co-expressed in the cell as YFP- and CFP-fusion proteins, or linked together in one hybrid molecule flanked by YFP and CFP. GTP loading of a GTPase alters FRET efficiencies between CFP and YFP owing to the interaction between the GTPase and an effector (Jiang and Sorkin, 2002; Kraynov et al., 2000) or conformational changes within the hybrid sensor (Mochizuki et al., 2001).

These FRET sensors have been used primarily to study small GTPases, such as Ras, Rap1 and Rac, participating in signal transduction. Hence, we developed a FRET-based assay to visualize the activity of Rab5, a GTPase that regulates endocytic trafficking. The design of the Rab5-GTP sensor (R5BD-YFP) was based on the information provided by in vitro experiments, which defined the part of Rabaptin5 molecule binding to Rab5 (Vitale et al., 1998). In FRET experiments, the expression of wild-type CFP-Rab5 or constitutively active CFP-Rab5 led to binding of a pool of R5BD-YFP to endosomes and an energy transfer from CFP-Rab5 to R5BD-YFP in endosomes. Comparable FRETN values were obtained for wild-type and the Q79L mutant of Rab5, suggesting that the architecture of the complexes of both Rab5 forms with effectors is similar.

The endosomal localization of R5BD-YFP, in the absence of heterologously expressed Rab5, would be an indicator of the endogenous GTP-bound Rab5. However, in our experiments, R5BD-YFP was not detected in endosomes in the absence of Rab5 overexpression in either A-431, HeLa or PAE cells (Fig. 1B). This could be because of low expression levels of endogenous Rab5 and/or competition of R5BD-YFP with endogenous Rabaptin5 and other Rab5-binding proteins for interaction with Rab5-GTP. Interestingly, R5BD-YFP

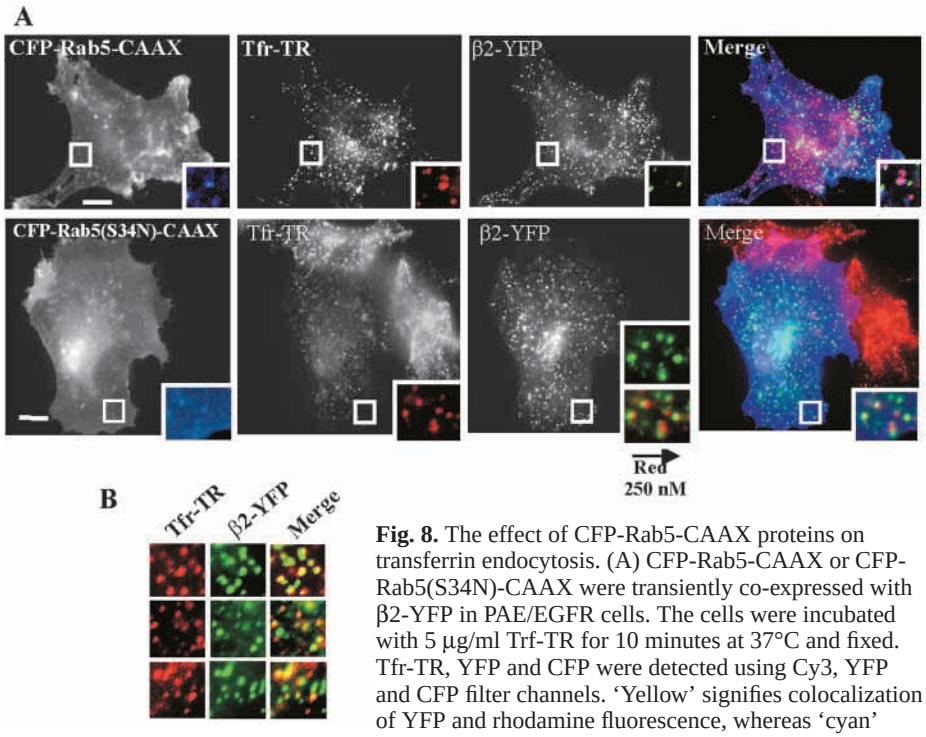

Fig. 8. The effect of CFP-Rab5-CAAX proteins on transferrin endocytosis. (A) CFP-Rab5-CAAX or CFP-Rab5(S34N)-CAAX were transiently co-expressed with β2-YFP in PAE/EGFR cells. The cells were incubated with 5 μg/ml Trf-TR for 10 minutes at 37°C and fixed. Tfr-TR, YFP and CFP were detected using Cy3, YFP and CFP filter channels. 'Yellow' signifies colocalization of YFP and rhodamine fluorescence, whereas 'cyan' signifies colocalization of CFP and rhodamine fluorescence. Insets show an enlargement of the outlined regions. Additional inset (low panel, YFP image) shows the merge image of Trf-TR and β2-YFP, in which the Trf-TR image (red) was right-shifted 4 pixels (250 nm) to allow better visualization of the overlap of red and green dots. The rhodamine image (low panel) is shown overexposed to visualize low levels of Trf-TR fluorescence in the cell expressing CFP-Rab5(S34N)-CAAX. This resulted in saturation of intense endosomal signals of Trf-TR in neighboring cells not expressing CFP-Rab5(S34N)-CAAX. Bar, 10 μM. (B) Gallery of high-magnification images from several cells expressing CFP-Rab5(S34N)-CAAX and treated as in (A) that show Tfr-TR colocalization with β2-YFP.

did localize to endosomes when CFP-EEA.1sh was also expressed (Fig. 1C). Presumably, the accumulation of CFP-EEA.1sh in endosomes elevated the concentration of GTP-loaded Rab5 in endosomes. This could be accomplished by driving the equilibrium between GTP- and GDP-bound forms of Rab5 towards GTP-binding through the direct interaction of Rab5-GTP with the EEA.1sh protein or indirectly, via other proteins of the fusion complex. This observation is consistent with a positive feedback mechanism involved in 'Rab5 microdomain' formation (Zerial and McBride, 2001).

Another Rab5-GTP sensor was generated on the basis of the Rab5-binding portion of the EEA.1 molecule (YFP-EEA.1sh). This probe was somewhat less useful for detecting the localization of active Rab5 because YFP-EEA.1sh localization in endosomes was dependent mainly on its FYVE domain rather than on the interaction with Rab5 (Dumas et al., 2001; Gaullier et al., 2000; Kutateladze and Overduin, 2001). However, this sensor was used for visualization of Rab5-GTP in active Rab5 microdomains, which were typically concentrated in sites of endosomal tethering and where FRET between Rab5 and EEA.1sh was especially evident (Fig. 3C). Rab5-R5BD complexes were also concentrated at fusion sites. However, FRET signals between Rab5 and R5BD were more equally distributed on the endosomal membrane and less enriched in the 'active domains' compared with the EEA.1 sensor, suggesting that the distribution of active Rab5 is not limited to the endosome fusion complexes. For instance, active Rab5 might be incorporated into Rabenosyn5-Rab4-Rab5 complexes outside of EEA.1-containing domains (de Renzis et al., 2002).

The FRET-based sensors, described above, are useful in the visualization of cellular localization of active GTP-bound Rab5 during signaling processes. In this regard, they are likely to be helpful in elucidating the in vivo functions of Rab5. In this work, we used the R5BD-YFP sensor to demonstrate the activity of Rab5-CAAX, a chimeric protein that was targeted to the plasma membrane (Fig. 5). This chimera was created to amplify the pool of Rab5 at the plasma membrane and to provide insight into the mechanisms by which Rab5 controls endocytosis through clathrin-coated pits. Earlier electron microscopy studies reported the detection of a small Rab5 pool at the plasma membrane (Chavrier et al., 1990). Studies using subcellular fractionation revealed the presence of Rab5 in clathrin-coated vesicles (Bucci et al., 1992). On the basis of in vitro organelle fusion experiments, it was proposed that a GDP-loaded Rab5(S34N) mutant inhibited endocytosis by blocking the fusion of coated vesicles with early endosomes (Bucci et al., 1992; Stenmark et al., 1994). However, other studies did not reveal the presence of endogenous or transfected Rab5 in coated vesicles (Barbieri et al., 2000). Also, the effect of Rab5(S34N) on internalization rates measured by the accessibility of ligand-receptor complexes to acidic wash stripping (Barbieri et al., 2000) is not consistent with the model that this mutant blocks the fusion step after the sequestration of complexes in coated vesicles. On the basis of the latter report and in vitro endocytosis assays, the hypothesis was put forward that Rab5 is involved in the receptor recruitment into coated pits (Barbieri et al., 2000) and/or coat assembly (McLauchlan et al., 1998).

In our experiments, EGF and transferrin receptors were efficiently recruited into coated pits in cells overexpressing Rab5(S34N) or Rab5(S34N)-CAAX, suggesting that Rab5 does not control early stages of endocytosis, such as coat assembly and cargo recruitment. Both dominant-negative Rab5 mutants prevented the movement of receptors from clathrin- and AP-2-positive structures to endosomes. Although we cannot formally rule out the possibility that these structures represent post-endocytic coated vesicles, we believe that these structures are coated pits. First, the pattern of distribution and the number of β2-YFP and YFP-CL_A positive dots per cell were essentially similar in cells expressing or not expressing Rab5 mutants. This pattern was qualitatively and quantitatively identical to the distribution of coated pits observed when receptors are accumulated in the coated areas under conditions restricting endocytosis at 4°C (Sorkina et al., 2002) or in the presence of the K44A mutant dynamin (Fig. 4B). Second, time-lapse imaging revealed that clathrin and AP-2-positive dots are virtually immobile (data not shown), which is a characteristic of coated pits but not of vesicles (Gaidarov et al., 1999). Third, the endocytosis process was blocked at a stage prior to clathrin uncoating, an event immediately following vesicle budding and necessary for fusion with endosomes. Since, to our knowledge, no data are available that implicate Rab5 or any other Rabs in the regulation of coat release, the block of endocytosis by Rab5 mutants is likely to occur upstream of the uncoating and fusion steps. Therefore, the inhibition of endocytosis by the Rab5 mutant at the stage of vesicle formation from coated pits is the most probable explanation for our data presented in Figs 4, 6-8. However, electron microscopy analysis would be necessary to determine the precise site of Rab5 mutant action.

The fact that Rab5(S34N)-CAAX mutant is an effective inhibitor of internalization suggested that GDP-bound Rab5 acts on clathrin-mediated endocytosis through sequestering regulators of Rab5, probably GEFs, or regulators common to Rab5 and other homologous Rab GTPases. Such regulators must be either cytosolic or associated with the plasma membrane rather than located on endosomal membranes. Our experiments also suggest that the inhibitory effect of the mutant is not mediated by Rab5-GDI because Rab5-CAAX is anchored to the membrane, lacks isoprenylation and is incapable of the interaction with Rab5-GDI (Sanford et al., 1995).

Interestingly, expression of constitutively active CFP-Rab5-CAAX resulted in extensive membrane motility. $FRET^C$ signals were detected mainly in numerous ruffles and pseudopodia, which are areas of increased actin cytoskeleton dynamics (Fig. 5). It is therefore possible that Rab5-GTP-CAAX recruits proteins involved in the regulation of cortical cytoskeleton dynamics (Jeng and Welch, 2001). For instance, phosphoinositide 3-kinases (PI3 kinases) are putative effectors of Rab5 (Li et al., 1995) and the elevated recruitment of PI3 kinases to the plasma membrane by Rab5-CAAX might increase PtdIns(3)*P* levels to effect actin polymerization locally. Overexpression of Rab5(Q79L) leads to acceleration of pinocytosis, a process that is associated with increased actin dynamics (Dharmawardhane et al., 1997; Lee and Knecht, 2002). The effects of Rab5(Q79L)-CAAX on membrane motility might be an amplification of similar effects of the analogous Rab5 mutant. Collectively, our experiments suggest that plasma-membrane-targeted Rab5 is capable of interaction with at least a subset of its regulators

and effectors. By contrast, effectors with strong targeting signals of their own, such as EEA.1, did not follow active Rab5-CAAX to the plasma membrane. Moreover, increased ruffling activity in cells overexpressing Rab5-CAAX might indicate that this chimeric protein binds to additional effectors specific to a plasma membrane Rab5 but not to endosomal Rab5.

In conclusion, we have established a new FRET-based assay for monitoring Rab5 activity in living cells that should be a useful tool for analyzing the localization of GTP-bound Rab5 in living cells. We also demonstrated that overexpression of a dominant-negative Rab5 mutant at the plasma membrane inhibits the late stages of clathrin-mediated endocytosis. Future studies will be necessary to define the molecular mechanisms and protein-protein interactions that underlie the possible role of Rab5 in this step of endocytosis.

We thank H. Stenmark, M. Zerial, M. McNiven, L. Krushel and L. Green for reagents and M. Dell'Acqua, R. Prekeris, K. Gleason and D. Port for critically reading the manuscript. This work was supported by grants CA089151 from NCI, RPG-00-247-01-CSM from ACS and MCB-0078509 grant from NSF.

References

Barbieri, M. A., Roberts, R. L., Gumusboga, A., Highfield, H., Alvarez-Dominguez, C., Wells, A. and Stahl, P. D. (2000). Epidermal growth factor and membrane trafficking. EGF receptor activation of endocytosis requires Rab5a. *J. Cell Biol.* **151**, 539-550.

Barbieri, M. A., Gumusboga, A., Roberts, R. L. and Stahl, P. D. (2001). Measurement of Rab5 protein kinase B/akt and regulation of ras-activated endocytosis. *Methods Enzymol.* **329**, 145-156.

Bucci, C., Parton, R. G., Mather, I. H., Stunnenberg, H., Simons, K., Hoflack, B. and Zerial, M. (1992). The small GTPase rab5 functions as a regulatory factor in the early endocytic pathway. *Cell* **70**, 715-728.

Ceresa, B. P., Lotscher, M. and Schmid, S. L. (2001). Receptor and membrane recycling can occur with unaltered efficiency despite dramatic Rab5(q79l)-induced changes in endosome geometry. *J. Biol. Chem.* **276**, 9649-9654.

Chavrier, P., Parton, R. G., Hauri, H. P., Simons, K. and Zerial, M. (1990). Localization of low molecular weight GTP binding proteins to exocytic and endocytic compartments. *Cell* **62**, 317-329.

Christoforidis, S. and Zerial, M. (2000). Purification and identification of novel Rab effectors using affinity chromatography. *Methods* **20**, 403-410.

Damke, H., Baba, T., Warnock, D. E. and Schmid, S. L. (1994). Induction of mutant dynamin specifically blocks endocytic coated vesicle formation. *J. Cell Biol.* **127**, 915-934.

de Renzis, S., Sonnichsen, B. and Zerial, M. (2002). Divalent Rab effectors regulate the sub-compartmental organization and sorting of early endosomes. *Nat. Cell Biol.* **4**, 124-133.

Dharmawardhane, S., Sanders, L. C., Martin, S. S., Daniels, R. H. and Bokoch, G. M. (1997). Localization of p21-activated kinase 1 (PAK1) to pinocytic vesicles and cortical actin structures in stimulated cells. *J. Cell Biol.* **138**, 1265-1278.

Dumas, J. J., Merithew, E., Sudharshan, E., Rajamani, D., Hayes, S., Lawe, D., Corvera, S. and Lambright, D. G. (2001). Multivalent endosome targeting by homodimeric EEA1. *Mol. Cell* **8**, 947-958.

Gaidarov, I., Santini, F., Warren, R. A. and Keen, J. H. (1999). Spatial control of coated-pit dynamics in living cells. *Nat. Cell Biol.* **1**, 1-7.

Gaullier, J. M., Simonsen, A., D'Arrigo, A., Bremnes, B., Stenmark, H. and Aasland, R. (1998). FYVE fingers bind PtdIns(3)*P*. *Nature* **394**, 432-433.

Gaullier, J. M., Ronning, E., Gillooly, D. J. and Stenmark, H. (2000). Interaction of the EEA1 FYVE finger with phosphatidylinositol 3-phosphate and early endosomes. Role of conserved residues. *J. Biol. Chem.* **275**, 24595-24600.

Gordon, G. W., Berry, G., Liang, X. H., Levine, B. and Herman, B. (1998). Quantitative fluorescence resonance energy transfer measurements using fluorescence microscopy. *Biophys. J.* **74**, 2702-2713.

Hahn, K. and Toutchkine, A. (2002). Live-cell fluorescent biosensors for activated signaling proteins. *Curr. Opin. Cell Biol.* **14**, 167-172.

Hancock, J. F., Paterson, H. and Marshall, C. J. (1990). A polybasic domain or palmitoylation is required in addition to the CAAX motif to localize p21ras to the plasma membrane. *Cell* **63**, 133-139.

Horiuchi, H., Lippe, R., McBride, H. M., Rubino, M., Woodman, P., Stenmark, H., Rybin, V., Wilm, M., Ashman, K., Mann, M. et al. (1997). A novel Rab5 GDP/GTP exchange factor complexed to Rabaptin-5 links nucleotide exchange to effector recruitment and function. *Cell* **90**, 1149-1159.

Jeng, R. L. and Welch, M. D. (2001). Cytoskeleton: actin and endocytosis – no longer the weakest link. *Curr. Biol.* **11**, R691-R694.

Jiang, X. and Sorkin, A. (2002). Coordinated traffic of Grb2 and Ras during epidermal growth factor receptor endocytosis visualized in living cells. *Mol. Biol. Cell* **13**, 1522-1535.

Jiang, X., Huang, F., Marusyk, A. and Sorkin, A. (2003). Grb2 regulates internalization of EGF receptor through clathrin-coated pits. *Mol. Biol. Cell* **14**, 858-870.

Kirchhausen, T. (2000). Three ways to make a vesicle. *Nat. Rev. Mol. Cell. Biol.* **1**, 187-198.

Kraynov, V. S., Chamberlain, C., Bokoch, G. M., Schwartz, M. A., Slabaugh, S. and Hahn, K. M. (2000). Localized Rac activation dynamics visualized in living cells. *Science* **290**, 333-337.

Kutateladze, T. and Overduin, M. (2001). Structural mechanism of endosome docking by the FYVE domain. *Science* **291**, 1793-1796.

Lanzetti, L., Rybin, V., Malabarba, M. G., Christoforidis, S., Scita, G., Zerial, M. and di Fiore, P. P. (2000). The Eps8 protein coordinates EGF receptor signalling through Rac and trafficking through Rab5. *Nature* **408**, 374-377.

Lawe, D. C., Patki, V., Heller-Harrison, R., Lambright, D. and Corvera, S. (2000). The FYVE domain of early endosome antigen 1 is required for both phosphatidylinositol 3-phosphate and Rab5 binding. Critical role of this dual interaction for endosomal localization. *J. Biol. Chem.* **275**, 3699-3705.

Lee, E. and Knecht, D. A. (2002). Visualization of actin dynamics during macropinocytosis and exocytosis. *Traffic* **3**, 186-192.

Li, G., D'Souza-Schorey, C., Barbieri, M. A., Roberts, R. L., Klippel, A., Williams, L. T. and Stahl, P. D. (1995). Evidence for phosphatidylinositol 3-kinase as a regulator of endocytosis via activation of Rab5. *Proc. Natl. Acad. Sci. USA* **92**, 10207-10211.

Lippe, R., Horiuchi, H., Runge, A. and Zerial, M. (2001). Expression, purification, and characterization of Rab5 effector complex, rabaptin-5/rabex-5. *Methods Enzymol.* **329**, 132-145.

Martinu, L., Santiago-Walker, A., Qi, H. and Chou, M. M. (2002). Endocytosis of epidermal growth factor receptor regulated by Grb2-mediated recruitment of the Rab5 GAP RN-tre. *J. Biol. Chem.* **277**, 50996-51002.

McLauchlan, H., Newell, J., Morrice, N., Osborne, A., West, M. and Smythe, E. (1998). A novel role for Rab5-GDI in ligand sequestration into clathrin-coated pits. *Curr. Biol.* **8**, 34-45.

Mochizuki, N., Yamashita, S., Kurokawa, K., Ohba, Y., Nagai, T., Miyawaki, A. and Matsuda, M. (2001). Spatio-temporal images of growth-factor-induced activation of Ras and Rap1. *Nature* **411**, 1065-1068.

Nielsen, E., Christoforidis, S., Uttenweiler-Joseph, S., Miaczynska, M., Dewitte, F., Wilm, M., Hoflack, B. and Zerial, M. (2000). Rabenosyn-5, a novel Rab5 effector, is complexed with hVPS45 and recruited to endosomes through a FYVE finger domain. *J. Cell Biol.* **151**, 601-612.

Prior, I. A., Harding, A., Yan, J., Sluimer, J., Parton, R. G. and Hancock, J. F. (2001). GTP-dependent segregation of H-ras from lipid rafts is required for biological activity. *Nat. Cell Biol.* **3**, 368-375.

Reuther, G. W. and Der, C. J. (2000). The Ras branch of small GTPases: Ras family members don't fall far from the tree. *Curr. Opin. Cell Biol.* **12**, 157-165.

Roberts, R. L., Barbieri, M. A., Pryse, K. M., Chua, M., Morisaki, J. H. and Stahl, P. D. (1999). Endosome fusion in living cells overexpressing GFP-rab5. *J. Cell Sci.* **112**, 3667-3675.

Roberts, R. L., Barbieri, M. A., Ullrich, J. and Stahl, P. D. (2000). Dynamics of rab5 activation in endocytosis and phagocytosis. *J. Leukoc. Biol.* **68**, 627-632.

Sanford, J. C., Yu, J., Pan, J. Y. and Wessling-Resnick, M. (1995). GDP dissociation inhibitor serves as a cytosolic acceptor for newly synthesized and prenylated Rab5. *J. Biol. Chem.* **270**, 26904-26909.

Sonnichsen, B., de Renzis, S., Nielsen, E., Rietdorf, J. and Zerial, M.

(2000). Distinct membrane domains on endosomes in the recycling pathway visualized by multicolor imaging of Rab4, Rab5, and Rab11. *J. Cell Biol.* **149**, 901-914.

Sorkin, A. and von Zastrow, M. (2002). Signal transduction and endocytosis: close encounters of many kinds. *Nat. Rev. Mol. Cell. Biol.* **3**, 600-614.

Sorkin, A., McClure, M., Huang, F. and Carter, R. (2000). Interaction of EGF receptor and grb2 in living cells visualized by fluorescence resonance energy transfer (FRET) microscopy. *Curr. Biol.* **10**, 1395-1398.

Sorkina, T., Huang, F., Beguinot, L. and Sorkin, A. (2002). Effect of tyrosine kinase inhibitors on clathrin-coated pit recruitment and internalization of epidermal growth factor receptor. *J. Biol. Chem.* **277**, 27433-27441.

Stenmark, H. and Olkkonen, V. M. (2001). The Rab GTPase family. *Genome Biol.* **2**, REVIEWS3007

Stenmark, H., Parton, R. G., Steele-Mortimer, O., Lutcke, A., Gruenberg, J. and Zerial, M. (1994). Inhibition of rab5 GTPase activity stimulates membrane fusion in endocytosis. *EMBO J.* **13**, 1287-1296.

Stenmark, H., Vitale, G., Ullrich, O. and Zerial, M. (1995). Rabaptin-5 is a direct effector of the small GTPase Rab5 in endocytic membrane fusion. *Cell* **83**, 423-432.

Vanderklish, P. W., Krushel, L. A., Holst, B. H., Gally, J. A., Crossin, K. L. and Edelman, G. M. (2000). Marking synaptic activity in dendritic spines with a calpain substrate exhibiting fluorescence resonance energy transfer. *Proc. Natl. Acad. Sci. USA* **97**, 2253-2258.

Vitale, G., Rybin, V., Christoforidis, S., Thornqvist, P., McCaffrey, M., Stenmark, H. and Zerial, M. (1998). Distinct Rab-binding domains mediate the interaction of Rabaptin-5 with GTP-bound Rab4 and Rab5. *EMBO J.* **17**, 1941-1951.

Zerial, M. and McBride, H. (2001). Rab proteins as membrane organizers. *Nat. Rev. Mol. Cell. Biol.* **2**, 107-117.

Zhang, J., Campbell, R. E., Ting, A. Y. and Tsien, R. Y. (2002). Creating new fluorescent probes for cell biology. *Nat. Rev. Mol. Cell. Biol.* **3**, 906-918.